ORIGINAL ARTICLE

Evaluating the Effect of Increasing Working Memory Load on EEG-Based Functional Brain Networks

Susan Samiei, Mehdi Delrobaei, Ali Khadem *

Department of Biomedical Engineering, Faculty of Electrical Engineering, K. N. Toosi University of Technology, Tehran, Iran

*Corresponding Author: Ali Khadem
Email: alikhadem@kntu.ac.ir

Received: 31 August 2021 / Accepted: 15 October 2021

Abstract

Purpose: Working Memory (WM) plays a crucial role in many cognitive functions of the human brain. Examining how the inter-regional connectivity and characteristics of functional brain networks modulate with increasing WM load could lead to a more in-depth understanding of the WM system.

Materials and Methods: To investigate the effect of WM load alterations on the inter-regional synchronization and functional network characteristics, we used Electroencephalogram (EEG) data recorded from 21 healthy participants during an n-back task with three load levels (0-back, 2-back, and 3-back). The networks were constructed based on the weighted Phase Lag Index (wPLI) in the theta, alpha, beta, low-gamma, and high-gamma frequency bands. After constructing the fully connected, weighted, and undirected networks, the node-to-node connections, graph-theory metrics consisting of mean Clustering coefficient (C), characteristic path Length (L), and node strength were analyzed by statistical tests.

Results: It was revealed that in the presence of WM load (2- and 3-back tasks) compared with the WM-free condition (0-back task) within the alpha range, the Inter-Regional Functional Connectivity (IRFC), functional integration, functional segregation, and node strength in channels located at the frontal, parietal and occipital regions were significantly reduced. In the high-gamma band, IRFC was significantly higher in the difficult task (3-back) compared to the easy and moderate tasks (0- and 2-back). Besides, locally clustered connections were significantly increased in 3-back relative to the 2-back task.

Conclusion: Inter-regional alpha synchronization and alpha-band network metrics can distinguish between the WM and WM-free tasks. In contrast, phase synchronization of high-gamma oscillations can differentiate between the levels of WM load, which demonstrates the potential of the phase-based functional connectivity and brain network metrics for predicting the WM load level.

Keywords: Electroencephalogram; Working Memory; Functional Connectivity; Weighted Phase Lag Index; Graph Theory.

DOI: https://doi.org/10.18502/fbt.v9i3.9641

1. Introduction

Working Memory (WM) refers to a short-term memory system that enables temporary storage, retrieval, and manipulation of information. The WM plays a vital role in the complex cognitive functions of the human brain, such as reasoning, problem-solving, language comprehension, and learning [1]. Increasing the difficulty level of WM-related tasks can increase the amount of load imposed on the WM system and affect cognitive performance [2]. The n-back task is a popular experimental paradigm for exploring WM function under varying difficulty levels. As n increases, the task becomes more difficult and the load imposed on WM increases [3]. Most of previous studies on WM have focused on the effect of the presence of or alteration in WM load on the hemodynamic activity of brain regions using functional Magnetic Resonance Imaging (fMRI) and functional Near-Infrared Spectroscopy (fNIRS) modalities. These studies have generally revealed load-dependent activation in the specific regions of prefrontal and parietal cortices during the n-back task [3-7].

Although brain activation-based analysis provides valuable information, a more precise comprehension of the WM system would not be attainable without brain connectivity analysis. Functional connectivity is generally defined as the temporal dependency of signals from different anatomical regions [8]. Phase-based connectivity analyses employing electrophysiological data are widely used in the literature due to their neurophysiological interpretation and fast computation speed. The idea of phase-based connectivity methods is that when neural populations communicate, their oscillatory processes, measured through the phase, become synchronized [9].

Numerous studies have revealed that spatially separated brain regions can be functionally related. This mechanism of the brain has inspired researchers to examine the brain as a complex network [10]. In graph theory, a powerful mathematical framework used to analyze complex networks, networks are represented as graphs. In terms of Electroencephalogram (EEG)-based functional networks, graph nodes are EEG electrodes, and edges are some measures of functional interaction between pairs of electrodes. The graph-theoretical measures describe the properties of the reconstructed functional networks, such as functional segregation, functional integration, and the importance of each brain region. Functional segregation is the ability of the brain to process information in distinct dense regions, known as clusters, while functional integration refers to the rapid combination of information from different regions [11].

Examining how the characteristics of functional brain networks modulate with increasing WM load can help us gain a more precise understanding of the WM system. A limited number of studies have explored this aspect in detail. For example, in a study conducted by Dai *et al.* (2017) n-back task with two difficulty levels (0- and 2-back) was employed, and the Pearson correlation coefficient between the EEG signals projected on the source space in the theta and alpha bands was calculated. The authors reported that, along with memory load increase, functional integration in the theta band increased, while functional segregation in the alpha band decreased [12]. In another study, Sun *et al.* (2019) used the Pearson correlation coefficient between the fNIRS channels to evaluate hemodynamic-based connectivity in the prefrontal cortex. Their results revealed that the length of the network paths was longer in the 2-back task than in the 0-back task [13]. To generalize the results of such studies, more load levels should be examined. Besides, an increasing number of findings suggest that high-frequency oscillations, especially high-gamma oscillations, play an important role in high-order cognitive processing involved in WM; accordingly, multi-frequency band analysis could lead to a more thorough understanding of the WM-related characteristics of brain networks [14-16].

In this study, we increased the number of load levels to three (0-back, 2-back, and 3-back). We used EEG data, weighted Phase Lag Index (wPLI) as a phase-based connectivity measure, and graph-theoretical metrics to investigate the effect of increasing WM load on inter-regional interactions and characteristics of functional cortical networks in the five frequency bands, including theta, alpha, beta, low-gamma, and high-gamma. To the best of our knowledge, the present study is the first study that has used wPLI employing EEG data to examine the effect of WM load-related alterations on functional connectivity.

The remainder of the paper is organized as follows. Section 2 describes dataset and data pre-processing. This section also explains our methodology, including brain functional network construction, graph local and global measures estimation, and statistical analyses. The experimental results are presented in section 3. Finally, Section 4 discusses the findings and Section 5 concludes the work.

2. Materials and Methods

2.1. N-back Dataset

In this work, we used an open-source dataset collected at the Technical University of Berlin by Shin *et al.* (2017) [17]. The data were recorded from 26 healthy right-handed participants who performed the n-back task at three load levels (conditions), including 0-back, 2-back, and 3-back. Data from five participants were excluded from further analysis due to relatively large noise. Thus, a total of 21 participants (16 females and 5 males) with a mean age of 28.86 ± 3.9 (mean ± standard deviation) years old were included in the data sample. The dataset consisted of three sessions, where one session contained three blocks of each condition. A total of 180 trials per condition were performed by each participant. In each trial, first, a random one-digit number was shown for 0.5 s. Then, the number disappeared, and a fixation cross appeared for 1.5 s. During this time, participants had to press the 'target' or 'non-target' button, according to the displayed number. Data were recorded using 28 EEG electrodes (plus ground and reference electrodes) according to the international 10-5 system with a sampling rate of 1000 Hz. Figure 1 depicts the location of EEG electrodes. For further details of the data acquisition protocol, please refer to reference section [17].

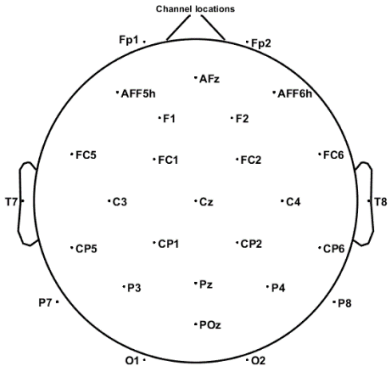

Figure 1. The location of EEG electrodes

2.2. Pre-Processing

The EEG data were pre-processed using EEGLAB toolbox (version 2020.0) running under MATLAB 2020a (MathWorks, CA, USA) [18]. First, a high-pass zero-phase Hamming-windowed sinc Finite Impulse Response (FIR) filter (cut-off frequency 0.5 Hz, transition bandwidth 1 Hz) was applied to continuous EEG data [19]. Next, data were re-referenced to the average of all EEG channels and were decomposed using Independent Component Analysis (ICA) based on the Adaptive Mixture ICA (AMICA) algorithm [20]. Common artifacts were identified by the ICLabel classifier and visually inspected based on their spectra, topography (spatial map), and time course [21]. Components corresponding to eye movements and muscle artifacts were removed. Further, a notch filter (zero-phase Hamming-windowed sinc FIR, cut-off frequencies 46 and 54 Hz, transition bandwidth 2 Hz) was applied to remove line noise. One sample of EEG signals before and after pre-processing is illustrated in Figure 2. Finally, the continuous data were segmented into epochs of -1 to 3 s following the stimulus onset. It should be noted that our time period of interest is from 0 to 2 s and these extra 1-s zones (i.e., from -1 to 0 s and also from 2 to 3 s relative to stimulus onset), which substantially reduce edge artifacts (high-amplitude

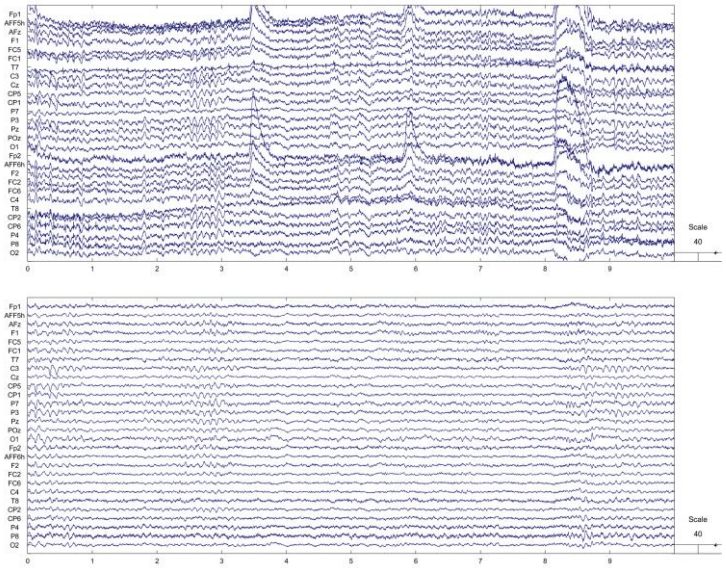

Figure 2. An example of raw (top plot) and pre-processed EEG signals (bottom plot)

broadband power artifacts resulting from time-frequency decomposition of sharp edges), would be cut after time-frequency decomposition [9].

2.3. Phase-Based Functional Connectivity Estimation

As mentioned earlier, wPLI was computed to estimate functional connectivity between each pair of electrodes. wPLI assesses the phase lagging consistency between two oscillating time series from two EEG channels. wPLI is an extension of the Phase Lag Index (PLI) in which phase differences further away from zero or π radians have a greater effect on the calculated connectivity value, resulting in wPLI being less sensitive to uncorrelated, volume-conducted noise sources. wPLI is computed as follows (Equation 1) [22].

$$wPLI = \frac{|E\{|I(S)|sgn(I(S))\}|}{E\{|I(s)|\}} \quad (1)$$

Where $I(S)$ is the imaginary part of the cross-spectrum and E{.} is the expected value operator. wPLI values range between zero (no phase consistency) and one (fully phase synchrony). Since wPLI ignores the zero and π phase differences, it is robust to spurious functional connectivity due to the volume conduction and active reference electrodes. Thus, it is a reliable estimator for EEG-based functional network construction. The cross-spectrum of each epoch was obtained by convolution of the time series signal with a set of complex Morlet wavelets with the Full Width at Half Maximum (FWHM) ranging from 150 to 500 ms [23]. Equation 1 was then used to calculate wPLI in 2-s (0 to 2 s) epochs. wPLI-based connectivity matrices were averaged across the theta (4-8 Hz), alpha (8-13 Hz), beta (13-30 Hz), low-gamma (30-50 Hz), and high-gamma (50-80 Hz) band and then averaged across epochs corresponding to each condition for each frequency band. As the estimation of the brain functional connectivity network metrics may highly depend on the chosen threshold value for binary connectivity matrix construction, no thresholding method was applied to the connectivity matrices. Therefore, we used 28×28 fully connected, weighted, and undirected functional connectivity matrices for the rest of the analyses [24, 25].

2.4. Graph Theory Metrics

After network construction, the topological differences of networks in three conditions of the n-back task were assessed by some graph-theoretical measures. There are many metrics in graph theory to describe the characteristics of a network, but not all of them are relevant for studying the cognitive functions of the brain. Here we considered a number of neurobiologically interpretable network metrics. These measures detect aspects of functional integration, functional segregation and quantify the importance of individual brain regions (centrality). Network measures were computed employing the Brain Connectivity toolbox [11]. The considered graph theory metrics are described in the following.

2.4.1. Characteristic Path Length (L)

The characteristic path Length (L), defined as the average of the shortest paths between all pairs of nodes, is the most commonly used measure of functional integration. This measure is inversely related to the brain's ability to rapidly combine pieces of specialized information from distributed brain regions. Generally, a short L indicates the effective integrity and rapid information propagation between the brain regions. In this study, L was computed as (Equation 2):

$$L = \frac{1}{n(n-1)} \sum_{i \in N} \sum_{j \in N, j \neq i} d_{ij} \quad (2)$$

In which *n* refers to the number of nodes, *N* is the set of all nodes in the network, and d_{ij} is the shortest weighted path (i.e., the inverse of wPLI) between node *i* and *j*.

2.4.2. Mean Clustering Coefficient (C)

The mean Clustering coefficient (C) of the network reflects, on average, the prevalence of clustered connectivity around individual nodes. Therefore, it generally shows functional segregation. The existence of clusters implies the presence of specific brain regions grouped to perform specialized processing. In this study, C was calculated as (Equation 3):

$$C = \frac{1}{n(n-1)\,(n-2)} \sum_{i \in N} \sum_{j,h \in N} (wPLI_{ij}\, wPLI_{ih}\, wPLI_{jh})^{\frac{1}{3}} \quad (3)$$

Where *n* is the number of nodes, and *N* is the set of all nodes in the network.

2.4.3. Node Strength

The node strength refers to the sum of weights of links connected to the node. Node strength is one of

the most common measures for centrality because it has a direct neurobiological interpretation: nodes with high node strength have a high functional association with other nodes in the network.

2.5. Statistical Analyses

In order to investigate the task difficulty-related differences on behavioral performance (accuracy and reaction time), a one-way Analysis of Variance (ANOVA) with repeated measures was performed. Post-hoc analysis was conducted using paired t-test with Bonferroni correction. A statistical significance threshold of 0.05 (p = 0.05) was selected for all statistical analyses performed in the present study.

Since the data did not meet the assumptions for normality or homogeneity of variance, Friedman test, which is a non-parametric test, was used to compare node-to-node wPLIs and network measures between conditions in all five studied frequency bands. The data were assessed for normality using the Shapiro-Wilk test and for homogeneity using the Levene test. Wilcoxon signed-rank tests were used for post-hoc pairwise comparisons with Bonferroni correction for the global measures (mean clustering coefficient and characteristic path length) and False Discovery Rate (FDR) adjustment for the local measure of networks (node strength) and inter-regional connectivity [26].

3. Results

3.1. Behavioral Results

Reaction time was obtained by computing the mean of the response times to the stimuli at each condition. One-way repeated measure ANOVA with a Greenhouse-Geisser correction indicated a significant main effect of memory load levels on reaction time (F (1.348, 26.966) = 138.022, $p < 10^{-12}$). Paired t-tests with Bonferroni correction revealed that reaction time significantly increased with increasing WM load (Table 1 and Figure 3A).

Table 1. Behavioral results: reaction time (ms) and accuracy (%) (mean ± standard deviation)

N-back task	Reaction time (ms)	Accuracy (%)
0-back	352 ± 71	98.9 ± 2.0
2-back	750 ± 171	91.6 ± 7.4
3-back	838 ± 185	82.8 ± 9.3

Also, accuracy was obtained by calculating the mean percentage of correct responses within each memory load condition. One-way repeated measure ANOVA with a Greenhouse-Geisser correction indicated a significant main effect of memory load levels on accuracy (F (1.396, 27.919) = 55.37, $p < 10^{-8}$). As expected, paired t-tests with Bonferroni adjustment revealed that accuracy significantly decreased with the increase of workload (Table 1 and Figure 3B).

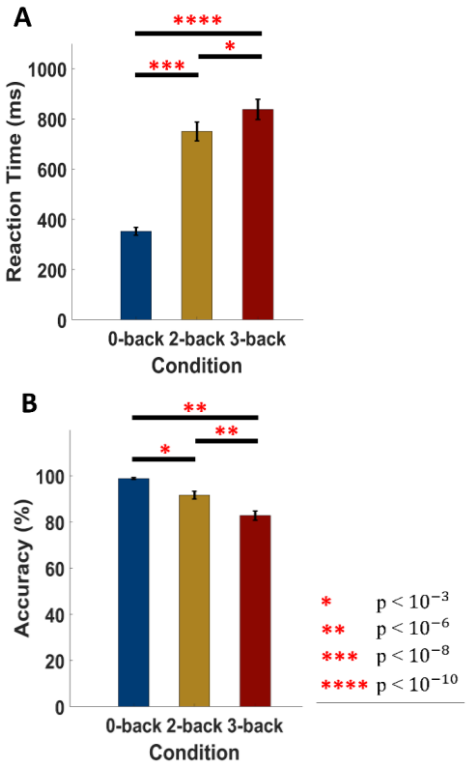

Figure 3. The effect of task difficulty on reaction time (A) and accuracy (B). Error bars show the standard error of the mean. Average reaction time significantly increased with the increase of task difficulty (A). Average accuracy significantly decreased with the increase of task difficulty (B)

3.2. Inter-Regional Functional Connectivity

The node-to-node connections that showed significantly different wPLI between the n-back tasks (FDR corrected, q < 0.05) are shown in Figure 4. The graphs were drawn on the brain maps with the BrainNet viewer toolbox [27].

In the alpha band, Inter-Regional Functional Connectivity (IRFC) was generally lower in the presence of workload (2- and 3-back conditions) compared to the absence of workload (0-back) (Figure 4A-B). Statistical analysis

revealed a significant alpha band IRFC decrease in 2-back compared to 0-back over frontal-central connections, including the AFz-Cz, AFz-CP2, F2-Cz, F2-CP1, Fp1-C4, Fp1-CP2, and FC2-CP1, frontal-parietal connections of AFF5h-POz, FC2-Pz, and Fp2-P4, frontal- and central-occipital links in F1-O1, AFF6h-O1, C3-O1, and CP5-O1, a central-parietal connection of P3-C4, with the decrease in intra frontal, central, and parietal connections of AFz-Fp2, AFz-FC2, Fp1-FC2, F1-FC2, Cz-Cp5, and P4-P8 (Figure 4A). Moreover, a significant decrease in IRFC of alpha band was found in 3-back relative to 0-back over frontal-parietal links, including the AFF5h-P7, AFF5h-POz, AFz-P7, Fp2-P7, and FC6-Pz, frontal-central connections of AFz-CP2, and FC6-C3, a central-parietal connection of C4-AFz, along with the decrease in intra frontal and parietal links of AFz-FC2, Fp2-FC1, and P7-POz (Figure 4B).

In the high-gamma band, IRFC was generally higher in the difficult task (3-back) relative to the easy and moderate tasks (0- and 2-back conditions) (Figure 4C-D). Statistical analysis indicated a significant high-gamma band IRFC increase in 3-back compared to 0-back over a frontal-central connection of FC5-CP2, along with a central-parietal connection in CP2-P4, also intra central links of C3-CP2, C3-CP6, and CP2-CP6 (Figure 4C). Furthermore, a significant high-gamma increase in IRFC was found in 3-back compared to 2-back over frontal- and temporal-parietal links, including the AFz-P3, AFz-P4, FC6- P8, and T8-P8, frontal-central and -temporal connections of AFz-C4, AFF6h-T8, and FC6-T8, also parietal- and occipital-central links in P7-CP6, and O1-CP6, along with the increase in intra frontal and parietal links of AFz-AFF6h, AFz-FC6, and P3-Pz (Figure 4D).

3.3. Network Characteristics

Significant workload-related alterations (following Bonferroni correction) in global network metrics are shown in Figure 5. In the alpha band network, in the presence of WM load (2- and 3-back tasks) compared with the load-free WM task (0-back), the L value, a measure inversely related to functional integration, significantly increased (Figure 5A), while C value, a measure of functional segregation, exhibited a statistically significant decrease (Figure 5B). In the high-gamma band network, the C value significantly increased only in the 3-back task relative to the 2-back task (Figure 5C).

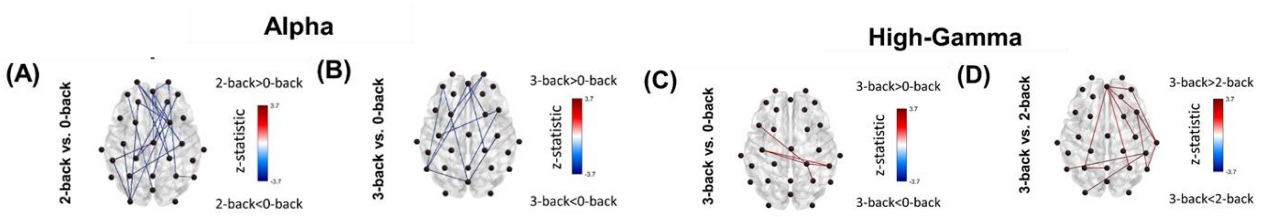

Figure 4. Connections with significant differences in wPLI between the n-back tasks (FDR corrected, $q < 0.05$) within the alpha range (A-B) and high-gamma band (C-D). The text on the left side of the figures indicates the type of tasks that were compared. The color bar represents the z-statistic obtained from Wilcoxon signed-rank test between the two tasks. The red links indicate a significant increase in synchronization, and the blue links show a significant decrease in synchronization with

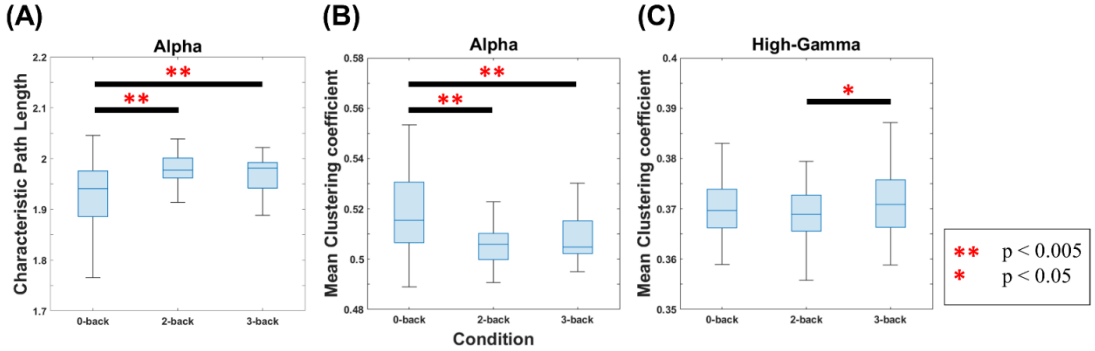

Figure 5. Significant workload-related alterations in global network metrics (following Bonferroni correction). Characteristic path length in the alpha band (A), mean clustering coefficient in the alpha band (B), mean clustering coefficient in high-gamma band (C). In the alpha-band, the 0-back condition could be identified with a significantly lower characteristic path length (A) and a higher mean clustering coefficient (B) than the 2- and 3-back WM tasks. In the high-gamma band, only a significant increase in the mean clustering coefficient value of 3-back compared to 2-back was observed (C). The boxplots show the 25th and 75th percentiles, median, and minimum and maximum values

Significant WM load-related changes in node strength are shown in Figure 6 and Table 2. In the alpha band, node strength decreased during increased mental workload in most of the channels. Our statistical analysis revealed a significant node strength decrease (after FDR correction for multiple comparisons, $q < 0.05$) within the alpha range in 2-back task relative to 0-back task across prefrontal channels, including the Fp1, Fp2, F1, F2, AFF5h, AFz, and FC2 also parietal channels of P4, P7, POz, and in left occipital O1 and right central C4. Furthermore, in the alpha band, a significant decrease in node strength values was found in 3-back task compared to 0-back task at frontal channels, including Fp1, Fp2, AFF5h, AFz, and FC6, parietal channels of P3, P4, P7, POz, and in both the left occipital O1 and right occipital O2 (Table 2).

4. Discussion

In this study, we investigated WM load-related alterations in phase-based IRFC and cortical network topology. The result of node-to-node connectivity analysis showed that the phase synchronization of alpha fluctuations in the presence of WM load (2- and 3-back tasks) was reduced compared to the condition without WM load (0-back task). Most of these differences were related to the interactions between the frontal and other regions, especially

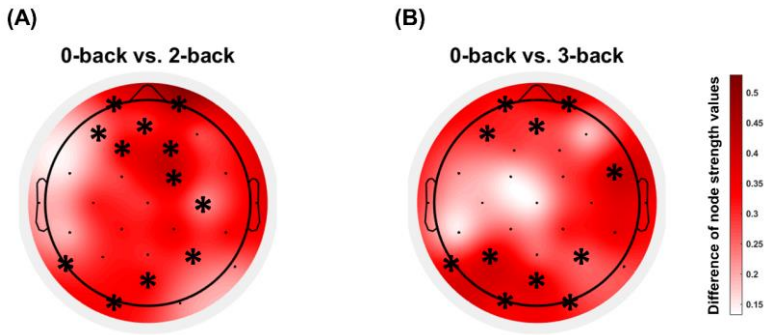

Figure 6. Significant WM load-related changes in node strength within the alpha band networks. "*" shows a significant difference (Wilcoxon signed-rank test) that remained after the FDR adjustment ($q < 0.05$). The color bar represents the difference of median values of node strength between the two conditions (0-back minus 2-back; 0-back minus 3-back). In the alpha band, node strength was generally lower in the presence of WM load (2- and 3-back conditions) relative to the WM load-free condition (0-back condition)

Table 2. EEG channels with significant differences (Wilcoxon signed-rank test) in node strength values between the n-back tasks (FDR corrected, $q < 0.05$) within the alpha range

EEG channel	Median of strength values			p-value	
	0-back	2-back	3-back	0- vs. 2-back	0- vs. 3-back
Fp1	14.00	13.66	13.67	0.0058	0.0058
Fp2	14.03	13.56	13.65	0.0079	0.0058
F1	13.89	13.53	13.61	0.0085	-
F2	14.01	13.61	13.73	0.0058	-
AFF5h	13.94	13.71	13.63	0.0058	0.0073
AFz	13.92	13.62	13.63	0.0058	0.0079
FC2	14.00	13.59	13.72	0.0058	-
FC6	13.98	13.67	13.57	-	0.0058
P3	14.03	13.73	13.65	-	0.0092
P4	13.98	13.70	13.72	0.0058	0.0073
P7	13.94	13.65	13.59	0.0098	0.0058
POz	14.09	13.75	13.72	0.0078	0.0058
O1	14.01	13.68	13.67	0.0073	0.0058
O2	14.02	13.80	13.71	-	0.0058
C4	13.98	13.76	13.66	0.0073	-

the parietal cortex (Figure 4A-B). These results are consistent with previous findings. For example, several studies demonstrated an opposite relationship between the number of items to be remembered (WM load) and the alpha power [28-30]. Also, Wianda *et al.* (2019) showed that regions with stronger Event-Related Synchronization (ERS) also exhibited stronger functional connectivity in a Sternberg WM task [31]. This inverse association between alpha power and mental workload in these trial-based paradigms suggests that as the WM load increases and the task becomes more difficult, the alpha oscillations will be relatively non-phase locked and less synchronized. In addition, we reported that phase synchronization was greater in the most difficult condition (3-back task) than the less difficult conditions (0- and 2-back tasks) within the high-gamma range. Most of the significant interactions were related to the connectivity between the frontal, parietal, and temporal areas, particularly in the 2-back vs. 3-back (Figure 4C-D). As mentioned earlier, WM involves the ability to maintain and manipulate information over a short duration of time. Synchronization of gamma oscillations has been discovered to be related to the maintenance of WM items [32, 33]. Besides, using Magnetoencephalography (MEG), Carver *et al.* (2019) revealed a stronger high-gamma power in the frontal, parietal, and temporal regions in the n-back conditions compared to rest, indicating synchronous high-gamma oscillations in high WM load conditions [14].

We utilized the tools provided by graph theory to examine the topological characteristics of the constructed functional networks. As demonstrated in Figure 5A, the L value of the 2- and 3-back WM tasks were higher than the control task (0-back) within the alpha range, suggesting the enhanced long-range connections and reduced functional integration. This increase in the L value can be explained by the decreased synchronization in the presence of workload and subsequently reduced weight of the graph edges (see the IRFC results and Equation 2). In addition, we found a decrease in the C value of alpha band network in the presence of WM load (Figure 5B). This result is consistent with a previous EEG study on WM that reported lower functional segregation in the 2-back task relative to the 0-back task within the alpha range [12]. As shown in Figure 5C, there was a significant enhancement in the C value from 2-back to 3-back task in the high-gamma band, indicating that the locally clustered connections were increased with the increasing load demand. Moreover, a significant reduction in node strength was observed at frontal, parietal, and occipital regions in the presence of workload within the alpha range (Figure 6A-B). In general, a significant difference between the node strength values of WM and WM-free tasks in the alpha band was expected since the IRFC corresponding to the mentioned regions were significantly different, the sum of them (i.e., strength) was also expected to be significantly different between the two types of tasks.

Our results suggest that phase synchronization between the alpha oscillations of the frontal-parietal regions can discriminate between the two conditions: with and without the workload, while phase synchronization between the high-gamma oscillations is more associated with high-level WM-related processing and can differentiate between the levels of WM load. Thus, an effective combination of the phase-based IRFC and graph-theoretical metrics in the alpha and high-gamma band networks can be explored as novel features for future Brain-Computer Interface (BCI) studies on mental workload classification. Furthermore, Cross Frequency Coupling (CFC), which refers to a statistical dependency between the amplitude or phase of a slower rhythm and the amplitude or phase of a higher frequency, could be explored between the alpha and high-gamma oscillations in the future studies [34].

There are some limitations in the current study. The unbalanced gender ratio (~3:1 female:male) might have biased our findings. Previous studies suggested that females outperform males in verbal WM tasks, while males outperform females on visuospatial WM tasks [35]. Also, Gao *et al.* (2018) revealed that men need more brain activations and higher EEG and fNIRS-based small world network properties to achieve similar performance as women do during verbal Sternberg tasks, suggesting that women surpass men in verbal WM tasks [36]. Therefore, the effect of gender must be taken into considerations in statistical analyses to obtain reliable results. In addition, the interpretability and generalizability of the reported results may be affected by the relatively small sample size (21 participants). Further investigations with a larger sample size would be necessary to confirm our findings. In spite of these limitations, our findings contribute to the understanding of WM load-related alterations in phase-based IRFC and cortical network topology.

5. Conclusion

In this study, we examined the inter-regional interactions and topological alterations of wPLI-based networks during an n-back task with three load levels within five frequency

ranges, including theta, alpha, beta, low-gamma, and high-gamma. Our findings reveal that inter-regional alpha synchronization and alpha-band network metrics can distinguish between the WM and WM-free tasks. In contrast, phase synchronization of high-gamma oscillations can differentiate between the levels of WM load, which demonstrates the potential of the phase-based functional connectivity and brain network metrics for predicting the WM load level. Taken together, these findings demonstrate that multi-frequency analysis of functional connectivity networks has the potential of providing a more detailed understanding of the WM system.

Acknowledgments

The authors would like to thank the Cognitive Sciences and Technologies Council of Iran for providing financial support.

References

1- A. Baddeley, "Working memory." *Curr. Biol.*, vol. 20, no. 4, pp. R136–R140, (2010).

2- S. A. Schapkin, G. Freude, P. D. Gajewski, N. Wild-Wall, and M. Falkenstein, "Effects of working memory load on performance and cardiovascular activity in younger and older workers." *Int. J. Behav. Med.*, vol. 19, no. 3, pp. 359–371, 2012.

3- A. M. Owen, K. M. McMillan, A. R. Laird, and E. Bullmore, "N-back working memory paradigm: A meta-analysis of normative functional neuroimaging studies." *Hum. Brain Mapp.*, vol. 25, no. 1, pp. 46–59, (2005).

4- D. J. Veltman, S. A. R. B. Rombouts, and R. J. Dolan, "Maintenance versus manipulation in verbal working memory revisited: an fMRI study." *Neuroimage*, vol. 18, no. 2, pp. 247–256, (2003).

5- D. E. Nee *et al.*, "A meta-analysis of executive components of working memory." *Cereb. cortex*, vol. 23, no. 2, pp. 264–282, (2013).

6- M. K. Yeung *et al.*, "Reduced frontal activations at high working memory load in mild cognitive impairment: near-infrared spectroscopy." *Dement. Geriatr. Cogn. Disord.*, vol. 42, no. 5–6, pp. 278–296, (2016).

7- F. A. Fishburn, M. E. Norr, A. V Medvedev, and C. J. Vaidya, "Sensitivity of fNIRS to cognitive state and load." *Front. Hum. Neurosci.*, vol. 8, p. 76, (2014).

8- M. P. Van Den Heuvel and H. E. H. Pol, "Exploring the brain network: a review on resting-state fMRI functional connectivity." *Eur. Neuropsychopharmacol.*, vol. 20, no. 8, pp. 519–534, (2010).

9- M. X. Cohen, *Analyzing neural time series data: theory and practice*. MIT press, (2014).

10- E. T. Bullmore and D. S. Bassett, "Brain graphs: graphical models of the human brain connectome." *Annu. Rev. Clin. Psychol.*, vol. 7, pp. 113–140, (2011).

11- M. Rubinov and O. Sporns, "Complex network measures of brain connectivity: uses and interpretations." *Neuroimage*, vol. 52, no. 3, pp. 1059–1069, (2010).

12- Z. Dai *et al.*, "EEG cortical connectivity analysis of working memory reveals topological reorganization in theta and alpha bands." *Front. Hum. Neurosci.*, vol. 11, p. 237, (2017).

13- J. Sun *et al.*, "Connectivity properties in the prefrontal cortex during working memory: a near-infrared spectroscopy study." *J. Biomed. Opt.*, vol. 24, no. 5, p. 51410, (2019).

14- F. W. Carver, D. Y. Rubinstein, A. H. Gerlich, S. I. Fradkin, T. Holroyd, and R. Coppola, "Prefrontal high gamma during a magnetoencephalographic working memory task." *Hum. Brain Mapp.*, vol. 40, no. 6, pp. 1774–1785, (2019).

15- I. Alekseichuk, Z. Turi, G. A. de Lara, A. Antal, and W. Paulus, "Spatial working memory in humans depends on theta and high gamma synchronization in the prefrontal cortex." *Curr. Biol.*, vol. 26, no. 12, pp. 1513–1521, (2016).

16- J. Yamamoto, J. Suh, D. Takeuchi, and S. Tonegawa, "Successful execution of working memory linked to synchronized high-frequency gamma oscillations." *Cell*, vol. 157, no. 4, pp. 845–857, (2014).

17- J. Shin, A. Von Lühmann, D.-W. Kim, J. Mehnert, H.-J. Hwang, and K.-R. Müller, "Simultaneous acquisition of EEG and NIRS during cognitive tasks for an open access dataset." *Sci. data*, vol. 5, p. 180003, (2018).

18- A. Delorme and S. Makeig, "EEGLAB: an open source toolbox for analysis of single-trial EEG dynamics including independent component analysis." *J. Neurosci. Methods*, vol. 134, no. 1, pp. 9–21, (2004).

19- A. Widmann, E. Schröger, and B. Maess, "Digital filter design for electrophysiological data–a practical approach." *J. Neurosci. Methods*, vol. 250, pp. 34–46, (2015).

20- J. A. Palmer, K. Kreutz-Delgado, and S. Makeig, "AMICA: An adaptive mixture of independent component analyzers with shared components." *Swart. Cent. Comput. Neursoscience, Univ. Calif. San Diego, Tech. Rep*, (2012).

21- L. Pion-Tonachini, K. Kreutz-Delgado, and S. Makeig, "ICLabel: An automated electroencephalographic independent component classifier, dataset, and website." *Neuroimage*, vol. 198, pp. 181–197, (2019).

22- M. Vinck, R. Oostenveld, M. Van Wingerden, F. Battaglia, and C. M. A. Pennartz, "An improved index of

phase-synchronization for electrophysiological data in the presence of volume-conduction, noise and sample-size bias." *Neuroimage*, vol. 55, no. 4, pp. 1548–1565, (2011).

23- M. X. Cohen, "A better way to define and describe Morlet wavelets for time-frequency analysis." *Neuroimage*, vol. 199, pp. 81–86, (2019).

24- I. Zakharov, T. Adamovich, A. Tabueva, V. Ismatullina, and S. Malykh, "The effect of density thresholding on the EEG network construction." in *Journal of Physics: Conference Series*, vol. 1727, no. 1, p. 12009, (2021).

25- M. Jalili, "Functional brain networks: does the choice of dependency estimator and binarization method matter?." *Sci. Rep.*, vol. 6, no. 1, pp. 1–12, (2016).

26- Y. Benjamini and Y. Hochberg, "Controlling the false discovery rate: a practical and powerful approach to multiple testing." *J. R. Stat. Soc. Ser. B*, vol. 57, no. 1, pp. 289–300, (1995).

27- M. Xia, J. Wang, and Y. He, "BrainNet Viewer: a network visualization tool for human brain connectomics." *PLoS One*, vol. 8, no. 7, p. e68910, (2013).

28- A. Gevins, M. E. Smith, L. McEvoy, and D. Yu, "High-resolution EEG mapping of cortical activation related to working memory: effects of task difficulty, type of processing, and practice." *Cereb. cortex (New York, NY 1991)*, vol. 7, no. 4, pp. 374–385, (1997).

29- F. Roux and P. J. Uhlhaas, "Working memory and neural oscillations: alpha–gamma versus theta–gamma codes for distinct WM information?." *Trends Cogn. Sci.*, vol. 18, no. 1, pp. 16–25, (2014).

30- K. Fukuda, I. Mance, and E. K. Vogel, "α power modulation and event-related slow wave provide dissociable correlates of visual working memory." *J. Neurosci.*, vol. 35, no. 41, pp. 14009–14016, (2015).

31- E. Wianda and B. Ross, "The roles of alpha oscillation in working memory retention." *Brain Behav.*, vol. 9, no. 4, p. e01263, (2019).

32- F. Roux, M. Wibral, H. M. Mohr, W. Singer, and P. J. Uhlhaas, "Gamma-band activity in human prefrontal cortex codes for the number of relevant items maintained in working memory." *J. Neurosci.*, vol. 32, no. 36, pp. 12411–12420, (2012).

33- O. W. Murphy, K. E. Hoy, D. Wong, N. W. Bailey, P. B. Fitzgerald, and R. A. Segrave, "Individuals with depression display abnormal modulation of neural oscillatory activity during working memory encoding and maintenance." *Biol. Psychol.*, vol. 148, p. 107766, (2019).

34- R. T. Canolty and R. T. Knight, "The functional role of cross-frequency coupling." *Trends Cogn. Sci.*, vol. 14, no. 11, pp. 506–515, (2010).

35- T. Li, Q. Luo, and H. Gong, "Gender-specific hemodynamics in prefrontal cortex during a verbal working memory task by near-infrared spectroscopy." *Behav. Brain Res.*, vol. 209, no. 1, pp. 148–153, (2010).

36- C. Gao, J. Sun, X. Yang, and H. Gong, "Gender differences in brain networks during verbal Sternberg tasks: A simultaneous near-infrared spectroscopy and electro-encephalography study." *J. Biophotonics*, vol. 11, no. 3, p. e201700120, (2018).